

Editorial

Deep Underground Earthquake Observation: Small to Moderate Earthquakes and Microearthquakes Identification

Chang Chen^{1,2}, Wentao Wan^{1,2}, Yun Wang^{1,2*}, Jingsong Liu^{1,2}, Hongyi Li^{1,2},

Qiangqiang Miao³, Yongsheng He³, Juan Qi⁴, Chao Wang⁵



1. MPMC Research Group, School of Geophysics and Information Technology, China University of Geosciences, Beijing 10083, China

2. State Key Laboratory of Geological Processes and Mineral Resources, China University of Geosciences, Beijing 10083, China

3. Institute of Engineering Protection, Engineering Research Institute of Academy of Military Sciences, Luoyang 471000, China

4. College of Electrical and Information Engineering, Anhui University of Science and Technology, Huainan 232001, China

5. Institute of Geochemistry, Chinese Academy of Sciences, Guiyang 550081, China

 Chang Chen: <https://orcid.org/0000-0002-6450-5249>;  Yun Wang: <https://orcid.org/0000-0002-7543-4677>

0 INTRODUCTION

Small to moderate earthquakes and microearthquakes occur widely and numerously (Luo, 2010), which contributes to the research of focal mechanism, faults and deep geodynamics (Li et al., 2023; Yi et al., 2020; Mori, 1991). It is of great significance for the focal mechanism solution of main shock and the distribution of coseismic activities (Meng et al., 2022; Zhang et al., 2021). For example, more than 1 800 small earthquakes ($M_s < 3.0$) occurred before $M_s 6.4$ Yangbi earthquake on May 21, 2021 (Fu et al., 2023; Chen J et al., 2022; Chen W K et al., 2022; Yang et al., 2022; Long et al., 2021), and stations at Zipingpu reservoir recorded 1 569 small earthquakes from August 16, 2004 to May 10, 2008, about 4 years before the Wenchuan earthquake (Yin et al., 2022). Due to weaker energy, lower signal-to-noise ratio (SNR), small to moderate earthquakes are difficult to be recognized from the background noise.

Compared to surface observation, the deep underground environment, which has lower ambient noise, will be beneficial for identify small to moderate earthquakes and microearthquakes (Rosat et al., 2018; Chen, 2010). With soft sediments on the shallow surface, seismic waves will experience frequency-dependent amplification and attenuation, that is, site effect. To clarify the influence of site effect, as early in 1960s, seismologists tried to analyze different surface wave components and their energy proportions through comparisons of the surface and boreholes (Chen et al., 2018; Niu et al., 2008; Douze, 1964). Abercrombie (1997) and discussed the characteristic and superposition of near-surface Q values and amplification based on observations of borehole and surface. However, the above researches are all limited to small borehole space with

high frequency geophones. Yamada and Horike (2007) only extended the frequency to 0.1–1.0 Hz, just because the environment of high temperatures and pressures in deep boreholes seriously affect accuracy and stability of the borehole instruments, and clamping and coupling designs for reducing resonance further increase the difficulty to the borehole observation. Therefore, using deep underground tunnels as laboratories or platforms can provide sufficient space and suitable temperature and pressure environment for seismic observations. Gaffet et al. (2003) recorded an earthquake occurred in India using the broadband seismometers deployed in the low-noise underground laboratory LSBB (Laboratoire Souterrain à Bas Bruit) in France, which was constructed based on the decommissioned nuclear missile system, and discussed the relation between magnetic and seismic data. De Luca et al. (1998) analyze the site effect with seismometers installed at different sites, and compared to seismic records measured in the LNGS (Laboratori Nazionali del Gran Sasso) underground laboratory in central Italy.

In this study, we carried out a deep underground and surface seismic observation in Huainan Deep Underground Laboratory (HDUL) located at a shutdown coal mine, proved the significant features of underground observation through 55 earthquakes with magnitudes less than 5, and discussed the underlying advantages of deep underground observations.

1 SYNCHRONOUS EARTHQUAKE OBSERVATION

Panyidong Coal Mine, belonging to Huaihe Energy Company Limited, is located in Huainan City, China, on the west side of Tanlu-Fault. After shutdown, huge space of underground tunnels and complete electricity and water supply systems are retained at subsurface, including auxiliary facilities at surface, which provides good conditions to establish HDUL and redundant underground tunnel of 870 m depth (altitude -848 m) for scientific experiments and researches (Wang et al., 2023; Chen C et al., 2022).

During January and May 2020, three CMG-40TDE broadband seismometers (bandwidth: 30 s-100 Hz, numbers N32/N49/N62) were installed in underground stations of HDUL;

*Corresponding author: wangyun@mail.gyig.ac.cn

© China University of Geosciences (Wuhan) and Springer-Verlag GmbH Germany, Part of Springer Nature 2024

Manuscript received December 22, 2023.

Manuscript accepted January 25, 2024.

the other one was installed on the surface as a reference station (number N85), as illustrated in Figures 1a–1d. Underground stations were set at the eastern end of the main tunnel. Surface station was placed inside a building. All seismometers were powered by 12V batteries, and their sampling rates were set to 50 sps (sample per second). Because the deep underground cannot receive GNSS signals directly, underground seismometers were timed on the surface before being transported to the underground.

2 DATA PROCESSING AND ANALYSIS

Although underground seismometers were timed on the surface, inevitable clock drifts still occurred during long-term recording. Therefore, time correction is an additional procedure for preprocessing underground records, which is carried out through the following steps: (a) shift the time records by the underground station step by step with an interval of 0.01 s; (b) calculate the cross-correlation coefficient between surface and underground records after shifting time; (c) select the shift time which is corresponding to maximum cross-correlation coefficient as the clock drift of the underground station.

2.1 Earthquakes in the Catalog

The earthquake catalog we use is obtained from the China Earthquake Networks Center and the National Earthquake Data Center. For different events, the records are filtered with different pass bands determined by time-frequency analysis. The underground and surface stations finally identified 55 and 25 events with magnitudes less than 5 respectively, corresponding to the catalog, as listed in Table S1. The events in the catalog are classified in different magnitude scales, including local

magnitude M_L , broadband body-wave magnitude m_b , and surface wave magnitude M_s .

For events with magnitudes less than 5 and epicentral distance less than 1 000 km, underground stations captured obviously more events than the surface station. Therefore, in the following we will focus on earthquakes of magnitude below 5. For quantitative comparison, we calculate SNR of each earthquake according to the formula $SNR = 10 \log(\text{signal/noise})$ (dB), and compare the surface and underground observations from magnitude, epicentral distance and dominant frequency band.

2.2 $0.1 < \text{Magnitude} < 1$

A total of 13 events with magnitudes below 1 were recorded by underground stations whereas none by surface station. These earthquakes have weak energy and high frequency. Their epicentral distances are small, with smallest of 143.90 km and largest of 360 km. Taking the earthquake event occurred at Weishan, Shandong as an example (magnitude: M_L 0.7, epicentral distance: 236.6 km, focal depth: 7 km), time-frequency spectrums obtained by continuous wavelet transform are compared in Figure 2, and theoretical arrival times of P- and S-wave calculated by iasp91 model are marked in the figures (Kennet and Engdahl, 1991). Weak high frequency signals could be seen at about 70 s in the underground records, which are almost submerged by the long-period noise with amplitude of 1 $\mu\text{m/s}$. SNRs got significantly improved after band-pass filtering (pass band: 1–6 Hz), and the peak ground velocity (PGV) is about 0.1 $\mu\text{m/s}$. The epicenter is nearly lying at the north of HDUL (the back azimuth 359.5°), so weak P-wave and S-wave both can be identified in the N component, while only S-wave can be seen in the E component.

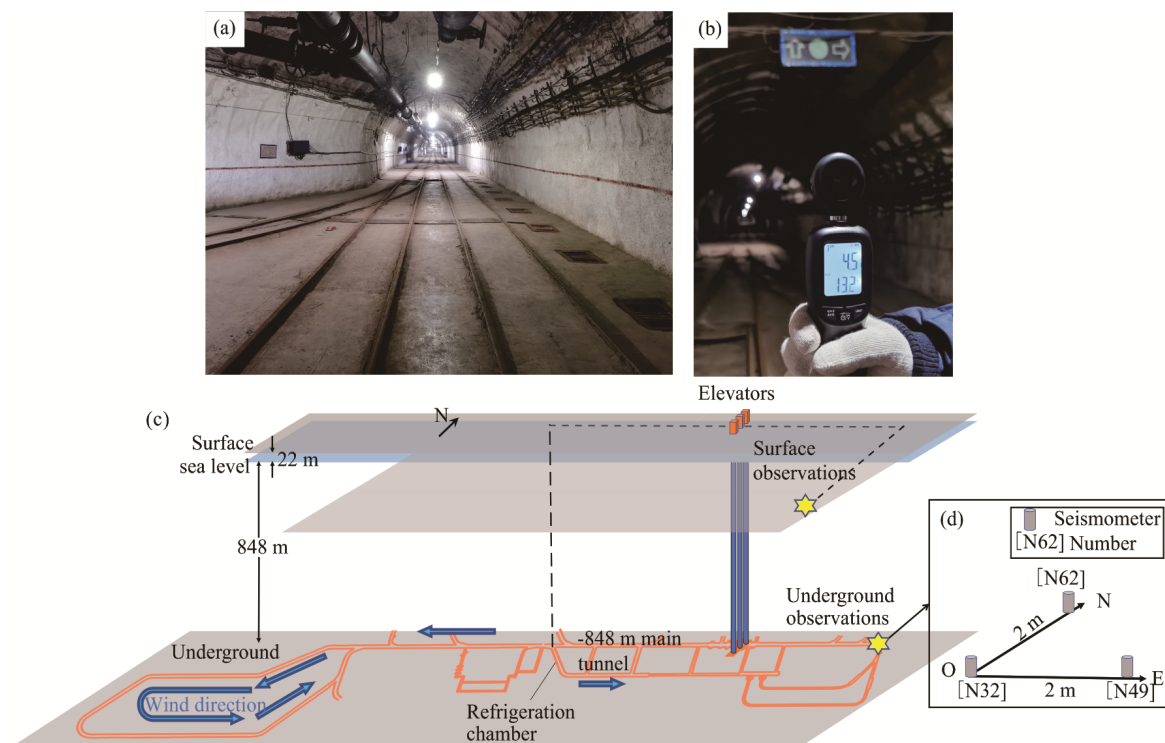


Figure 1. (a) Photo of underground tunnel; (b) temperature of underground main tunnel is about 13.2 °C, speed of wind produced by the ventilation system is about 4.5 m/s; (c) surface and underground observation station positions; (d) three seismometers were placed in 'L' shape at underground station.

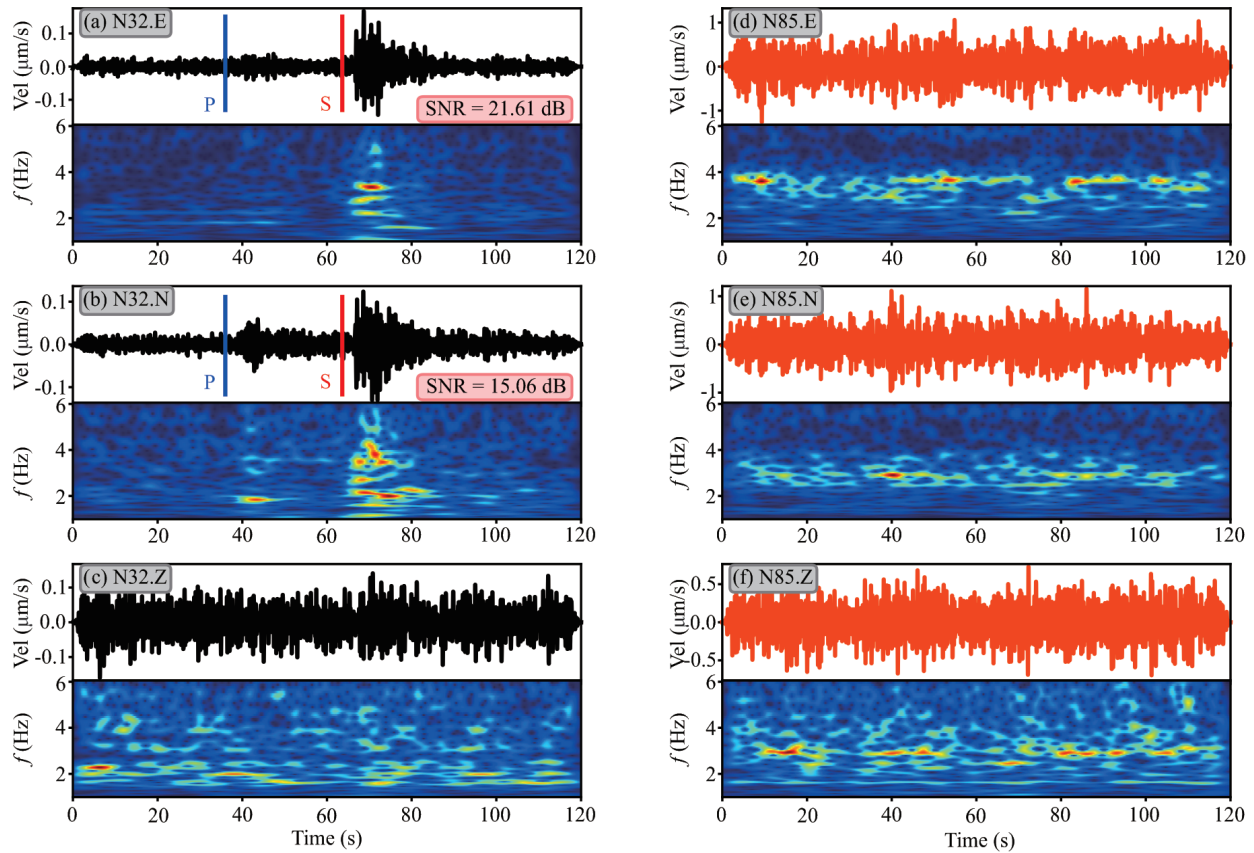


Figure 2. Three-component waveforms and time-frequency spectrums of E08 earthquake (band-pass filter: 1–6 Hz). (a)–(c) are E-/N-/Z- components recorded by N32 station in the underground, respectively; (d)–(f) are E-/N-/Z- components recorded by N85 station on the surface, respectively.

2.3 $1 \leq \text{Magnitude} < 4$

The underground stations captured 19 earthquakes with magnitudes between 1 and 4, with the minimum epicentral distance of 259.35 km and the maximum one 1 249.72 km. Among them, 9 earthquakes cannot be identified on the surface records, which are all small earthquakes with the maximum magnitude of $M_{2.2}$ and epicenter distance of 414.73 km; and they are characterized similarly to the earthquakes below M_1 , namely, their epicentral distances are small and energies are weak, mainly S-wave and surface wave. For the other 10 earthquakes that can be identified in both the surface and underground records, SNRs of the underground are generally higher than the surface. An example is E29 earthquake occurred in the Yellow Sea (magnitude: $M_{3.2}$, epicentral distance: 412.44 km, focal depth: 5 km), its 3-component velocity waveforms and Fourier amplitude spectrums are compared in Figure S1, which indicates that the dominant frequency is about 1–4 Hz. It's obviously that the waveforms recorded at the surface are markedly amplified because of the site effect, especially in the horizontal components (Chen et al., 2018). But affected by higher ambient noise, SNRs of the surface records are lower than that observed underground.

2.4 $4 \leq \text{Magnitude} < 5$

The underground stations captured 23 earthquakes with magnitudes between 4 and 5, 15 of which can be identified by surface observation. These earthquakes occurred widely in the epicentral distance of 1 000–8 000 km can be divided into two

categories.

Category A: Main wave mode is surface wave. These events have relatively shallow sources and low dominant frequency, usually below 1 Hz. Affected by the site effect, amplitudes of waveforms observed by the surface station are significantly amplified, so SNRs of surface records were generally higher than that of the underground. For example, we recorded an earthquake occurred in Lixian, Sichuan (magnitude: $M_{4.6}$, epicentral distance: 1 305.65 km, focal depth: 20 km), as shown in Figure S2. In both surface and underground records, body waves cannot be identified because surface wave with dominant frequency of 0.1–1 Hz is significantly strong. PGVs of the surface records are 5 times larger than the underground records, and SNRs of E and N components of the surface records are 29.70 and 22.29 dB, respectively, which are higher than 13.24 and 13.65 dB of the underground.

Category B: Main wave mode is P-wave. These events have relatively deep sources and high dominant frequency, usually above 1 Hz. Surface waves excited by these earthquakes are very weak and easily submerged by the self-noise of seismometers or environmental noises, while P-wave is easier to be highlighted. Therefore, the surface observations show as lower SNR and are difficult to be used to identify reliable events, such as E52 illustrated in Figure S3. Owing to low ambient noise, P-waves of these earthquakes are easily identified in the underground horizontal records with their SNRs 2–3 times higher than the surface records.

2.5 SNRs

The numbers of identified events classified by magnitude and its azimuth are illustrated in Figures 3a, 3b. For further quantitative comparison, SNRs of all 55 earthquake records below $M5$ are calculated and shown in Figure 3c, compared with magnitude, frequency and epicentral distance distributions in Figures 3d–3f. It can be statistically deduced that: (1) A total of 30 earthquakes can only be captured underground, mostly are small earthquakes below $M3$; (2) among the events identified on the surface records, the minimum magnitude is $M1.6$; (3) the underground stations captured 55 earthquakes below $M5$, while surface station only captured 25. In addition, among 26 earthquakes with epicentral distance less than 1 000 km identified by underground stations, only 4 can be identified synchronously by surface station, which indicates that the preponderances of underground stations are mainly manifested in the identification of earthquakes with magnitudes less than 5 or epicentral distance less than 1 000 km; (4) among 25 earthquakes that can be identified both on the surface and the underground, there are 13 earthquakes, which show as higher

SNRs at the surface. The main frequency centers of these 13 earthquakes were all less than 1 Hz (Figure 3e), and the amplitudes were significantly amplified due to site effect, which contributes to the higher SNRs.

3 DISCUSSION

3.1 Low-Noise Environment and Underlying Applications

Benefiting from absorption and attenuation of the thick cover, high-frequency noises from the surface or shallow medium affect little on underground observation. The comparison of ambient noise shows that the average noise amplitude of the surface records is about 14–30 times that of the underground, indicating underlying applications of underground laboratory, such as improving SNR and providing platforms for the testing of high-precision seismometers. On the other hand, the low-noise advantage would provide better environment to capture weak PcP and ScS signals reflected at the core-mantle boundary (Ni et al., 2018), and contribute to the exploration of deep structure and dynamic process of the earth.

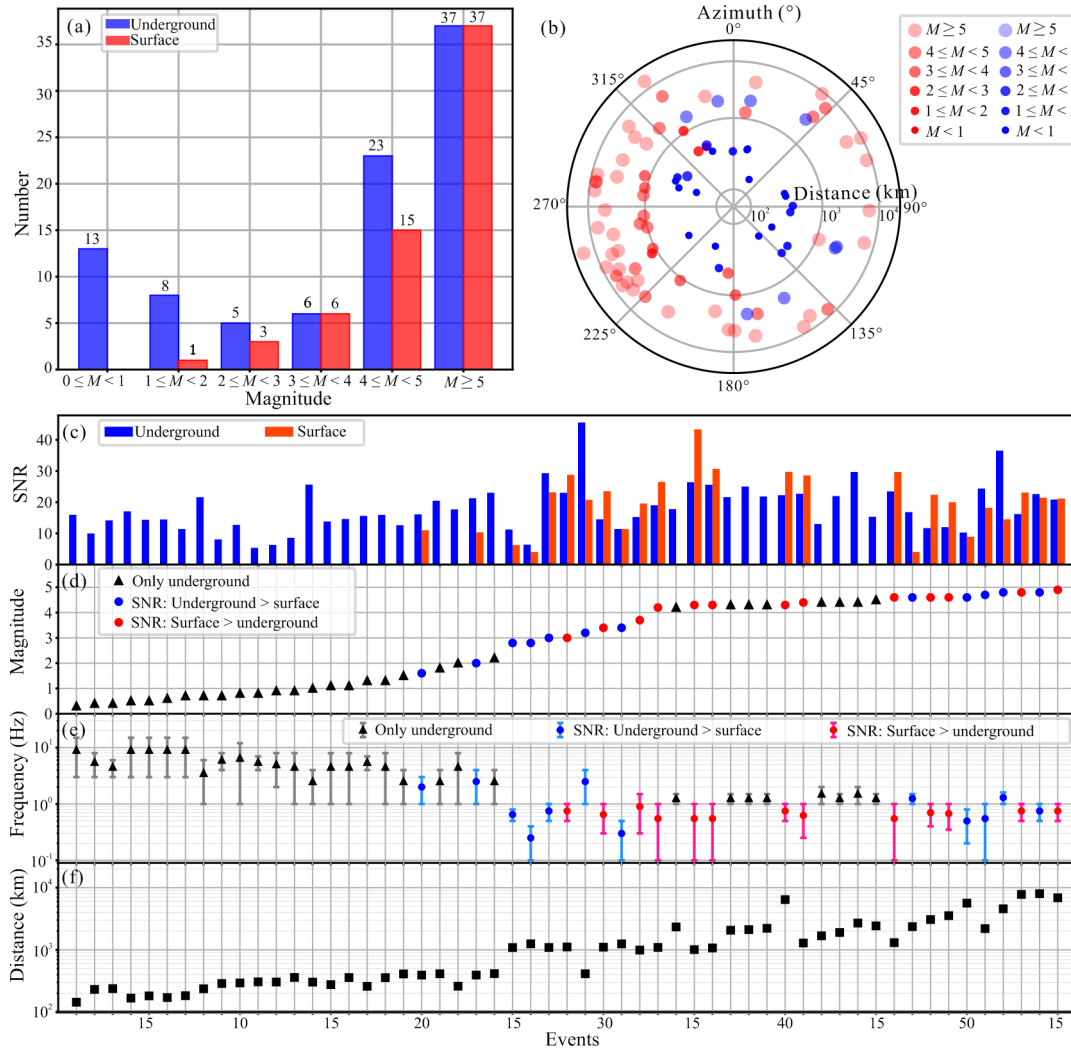


Figure 3. Earthquakes observed by underground and surface stations. (a) Number of identified events classified by magnitude; (b) azimuth and epicentral distance distribution of each event; (c) the SNRs of seismic records measured by underground and surface stations; (d) magnitude of each event; (e) dominant frequency of each event, the triangles and circles are center frequency, error bars denote the upper and lower bounds of the frequency band; (f) epicentral distance of each event.

3.2 Frequency-Dependent Site Effect

The site effect brings both amplification and attenuation for signals in different frequency band (Chen et al., 2018; Abercrombie, 1997). Further synchronous observation and research in HDUL can possibly distinguish distinct characteristics of amplification and attenuation, explore underlying mechanism of the site effect, and provide reference for magnitude correction for surface seismic observations.

3.3 Comparison to Borehole Observations

The borehole observations must face challenges of narrow space, high temperature and pressure, and the coupling of instruments, which would reduce the stability of observations and increase resonance. Deep underground laboratories could provide an extended space with proper temperature and pressure for observations, and enable the installation of large-size seismometers for recording long-period signals and rotational motions, such as broadband seismometers arrays, fiber-optic rotational seismometers, and Ring Laser Gyroscopes (Chen et al., 2023; Wang et al., 2022; Simonelli et al., 2016; Gaffet et al., 2003).

4 CONCLUSION

Affected by amplification and attenuation of the site effect, SNRs of records at the surface appear to be significantly frequency-dependent. For earthquakes with small magnitudes and epicentral distance, high-frequency S-wave and surface wave are easily identified in the underground records, and their SNRs are normally higher than the surface records. For remote earthquakes with main wave mode of low-frequency surface wave, SNRs of the surface records are higher because of amplification of the site effect. But for remote earthquakes excited by deep sources, as the main wave mode is confirmed as P-wave with frequency above 1 Hz, the underground records show as higher SNRs. Synchronous observations in HDUL show advantages in identifying small to moderate earthquakes and microearthquakes, especially the high-frequency signals above 1 Hz.

ACKNOWLEDGMENTS

This research is supported by the National Natural Science Foundation of China (Nos. 62127815, 42150201, U1839208, 41874166) and the Guizhou Science and Technology Cooperation Platform Talents Fund (No. [2021]5629). The final publication is available at Springer via <https://doi.org/10.1007/s12583-023-1962-8>.

Electronic Supplementary Materials: Supplementary materials (Figures S1, S2, S3; Table S1) are available in the online version of this article at <https://doi.org/10.1007/s12583-023-1962-8>.

Conflict of Interest

The authors declare that they have no conflict of interest.

REFERENCES CITED

Abercrombie, R. E., 1997. Near-Surface Attenuation and Site Effects from Comparison of Surface and Deep Borehole Recordings. *Bulletin of the*

Seismological Society of America, 87(3): 731–744. <https://doi.org/10.1785/bssa0870030731>

Chen, C., Wang, Y., Guo, G., et al., 2022. Deep Underground Observation Comparison of Rotational Seismometers. *Chinese Journal of Geophysics*, 65(12): 4569–4582 (in Chinese with English Abstract)

Chen, C., Wang, Y., Sun, L., et al., 2023. Six-Component Earthquake Synchronous Observations Across Taiwan Strait: Phase Velocity and Source Location. *Earth and Space Science*, 10(12): e2023ea003040. <https://doi.org/10.1029/2023ea003040>

Chen, H. C., Tsai, V. C., Niu, F. L., 2018. Observations and Modeling of Long-Period Ground-Motion Amplification across Northeast China. *Geophysical Research Letters*, 45(12): 5968–5976. <https://doi.org/10.1029/2018gl078212>

Chen, H. S., 2010. Deep Underground Sciences in China: Status and Prospects. *Bulletin of National Natural Science Foundation of China*, 24(2): 65–69 (in Chinese with English Abstract)

Chen, J., Tang, H., Chen, W. K., et al., 2022. A Prediction Method of Ground Motion for Regions without Available Observation Data (LGB-FS) and Its Application to both Yangbi and Madoo Earthquakes in 2021. *Journal of Earth Science*, 33(4): 869–884. <https://doi.org/10.1007/s12583-021-1560-6>

Chen, W. K., Wang, D., Zhang, C., et al., 2022. Estimating Seismic Intensity Maps of the 2021 *M*_w 7.3 Madoi, Qinghai and *M*_w 6.1 Yangbi, Yunnan, China Earthquakes. *Journal of Earth Science*, 33(4): 839–846. <https://doi.org/10.1007/s12583-021-1586-9>

De Luca, G., Del Pezzo, E., Di Luccio, F., et al., 1998. Site Response Study in Abruzzo (Central Italy): Underground Array Versus Surface Stations. *Journal of Seismology*, 2(3): 223–236. <https://doi.org/10.1023/a:1009786605055>

Douze, E. J., 1964. Rayleigh Waves in Short-Period Seismic Noise. *Bulletin of the Seismological Society of America*, 54(4): 1197–1212. <https://doi.org/10.1785/bssa0540041197>

Fu, G. Y., Wang, Z. Y., Liu, J. S., et al., 2023. Lithospheric Equilibrium and Anisotropy around the 2021 Yangbi *M*_s 6.4 Earthquake in Yunnan, China. *Journal of Earth Science*, 34(4): 1165–1175. <https://doi.org/10.1007/s12583-022-1607-3>

Gaffet, S., Guglielmi, Y., Virieux, J., et al., 2003. Simultaneous Seismic and Magnetic Measurements in the Low-Noise Underground Laboratory (LSBB) of Rustrel, France, during the 2001 January 26 Indian Earthquake. *Geophysical Journal International*, 155(3): 981–990. <https://doi.org/10.1111/j.1365-246x.2003.02095.x>

Kennett, B. L. N., Engdahl, E. R., 1991. Traveltimes for Global Earthquake Location and Phase Identification. *Geophysical Journal International*, 105(2): 429–465. <https://doi.org/10.1111/j.1365-246x.1991.tb06724.x>

Li, Y. Z., Li, H. Y., Huang, Y. F., et al., 2023. Micro-Earthquake Seismicity and Tectonic Significance of the 2012 *M*_s 4.9 Baoying Earthquake, Jiangsu, China. *Journal of Earth Science*, 34(3): 900–910. <https://doi.org/10.1007/s12583-022-1780-4>

Long, F., Qi, Y., Yi, G., et al., 2021. Relocation of the *M*_s 6.4 Yangbi earthquake Sequence on May 21, 2021 in Yunnan Province and Its Seismogenic Structure Analysis. *Chinese Journal of Geophysics*, 64(8): 2631–2646 (in Chinese with English Abstract)

Luo, Y., 2010. Source Parameters Study of Small to Moderate Earthquakes: [Dissertation]. University of Science and Technology of China, Hefei (in Chinese with English Abstract)

Meng, X., Ravanelli, M., Komjathy, A., et al., 2022. On the North-South Asymmetry of Co-Seismic Ionospheric Disturbances during the 16 September 2015 Illapel *M*_{8.3} Earthquake. *Geophysical Research*

- Letters*, 49(8): e98090. <https://doi.org/10.1029/2022gl098090>
- Mori, J., 1991. Estimates of Velocity Structure and Source Depth Using Multiple *P* Waves from Aftershocks of the 1987 Elmore Ranch and Superstition Hills, California, Earthquakes. *Bulletin of the Seismological Society of America*, 81(2): 508–523. <https://doi.org/10.1785/bssa0810020508>
- Ni, S., Zhou, Y., Qian, Y., et al., 2018. Did the Core Phase ScS of the Wenchuan Earthquake Trigger Its First M6 Aftershock? *AGU Fall Meeting Abstracts*, 2018: S14B-06
- Niu, F. L., Silver, P. G., Daley, T. M., et al., 2008. Preseismic Velocity Changes Observed from Active Source Monitoring at the Parkfield SAFOD Drill Site. *Nature*, 454: 204–208. <https://doi.org/10.1038/nature07111>
- Rosat, S., Hinderer, J., Boy, J. P., et al., 2018. A Two-Year Analysis of the IOSG-24 Superconducting Gravimeter at the Low Noise Underground Laboratory (LSBB URL) of Rustrel, France: Environmental Noise Estimate. *Journal of Geodynamics*, 119: 1–8. <https://doi.org/10.1016/j.jog.2018.05.009>
- Simonelli, A., Belfi, J., Beverini, N., et al., 2016. First Deep Underground Observation of Rotational Signals from an Earthquake at Teleseismic Distance Using a Large Ring Laser Gyroscope. *Annals of Geophysics*, 59: 1. <https://doi.org/10.4401/ag-6970>
- Wang, Y., Yang, Y. X., Sun, H. P., et al., 2023. Observation and Research of Deep Underground Multi-Physical Fields—Huainan -848 m Deep Experiment. *Science China Earth Sciences*, 66(1): 54–70. <https://doi.org/10.1007/s11430-022-9998-2>
- Yamada, K., Horike, M., 2007. Inference of Q-Values below 1 Hz from Borehole and Surface Data in the Osaka Basin by Three-Component Waveform Fitting. *Bulletin of the Seismological Society of America*, 97(4): 1267–1278. <https://doi.org/10.1785/0120040199>
- Yang, T., Li, B., Fang, L. H., et al., 2022. Relocation of the Foreshocks and Aftershocks of the 2021 Ms 6.4 Yangbi Earthquake Sequence, Yunnan, China. *Journal of Earth Science*, 33(4): 892–900. <https://doi.org/10.1007/s12583-021-1527-7>
- Yi, G., Zhou, L., Zhang, L., et al., 2020. Predictive Efficiency Tests of Moderate Earthquakes with Sizes $M_s \geq 4.5$ in Low Seismicity Regions within Sichuan Basin. *J. Seismol. Res.*, 262–269 (in Chinese with English Abstract)
- Yin, D., Dong, P., Shi, Y., 2022. Coulomb Stress Changes Induced by Small Earthquakes in the Zipingpu Reservoir Area and Its Significance to the Wenchuan Earthquake. *Chinese Journal of Geophysics*, 65(1): 256–267 (in Chinese with English Abstract)
- Zhang, K., Gan, W., Liang, S., et al., 2021. Coseismic Displacement and Slip Distribution of the 2021 May 21, M_s 6.4, Yangbi Earthquake Derived from GNSS Observations. *Chinese Journal of Geophysics*, 64(7): 2253–2266 (in Chinese with English Abstract)

(Responsible Editor: Jun Lu)